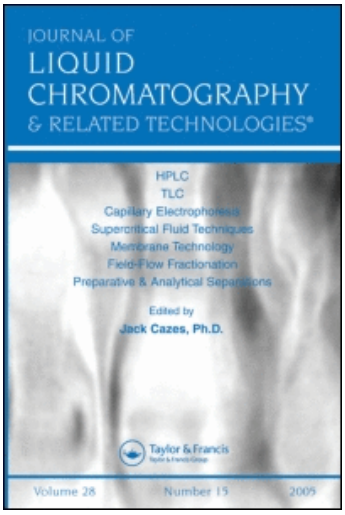

Journal of Liquid Chromatography & Related Technologies
Publication details, including instructions for authors and subscription information:
http://www.informaworld.com/smpp/title~content=t713597273

Elimination of the Interference from Nitrate Ions on Oxalic Acid in RP-HPLC by Solid-Phase Extraction with Nanosized Hydroxyapatite

Wei Wei[a]; Rong Sun[a]; Zhenggui Wei[a]; Haiyan Zhao[a]; Huixin Li[a]; Feng Hu[a]
[a] College of Resources and Environmental Sciences, Nanjing Agricultural University, Nanjing, P. R. China

To cite this Article Wei, Wei , Sun, Rong , Wei, Zhenggui , Zhao, Haiyan , Li, Huixin and Hu, Feng(2009) 'Elimination of the Interference from Nitrate Ions on Oxalic Acid in RP-HPLC by Solid-Phase Extraction with Nanosized Hydroxyapatite', Journal of Liquid Chromatography & Related Technologies, 32: 1, 106 — 124
To link to this Article: DOI: 10.1080/10826070802548705
URL: http://dx.doi.org/10.1080/10826070802548705

Journal of Liquid Chromatography & Related Technologies®, 32: 106–124, 2009

ISSN: 1082-6076 print/1520-572X online
DOI: 10.1080/10826070802548705

Elimination of the Interference from Nitrate Ions on Oxalic Acid in RP-HPLC by Solid-Phase Extraction with Nanosized Hydroxyapatite

Wei Wei, Rong Sun, Zhenggui Wei, Haiyan Zhao, Huixin Li, and Feng Hu

College of Resources and Environmental Sciences, Nanjing Agricultural University, Nanjing, P. R. China

Abstract: A new method using solid phase extraction with nanosized hydroxyapatite for solving interference from nitrate ions on oxalic acid in reversed phase high performance liquid chromatography (RP-HPLC) was developed. The optimum experimental conditions for the separation and determination of oxalic acid were studied. After the interference was eliminated, oxalic acid was determined by RP-HPLC at the optimum chromatographic conditions with an average recovery ranging between 94.8% and 99.3%, and the relative standard deviations were less than 3.0%. This method was successfully applied to determine the oxalic acid in the xylem saps of tomato.

Keywords: Determination, HPLC, Interference elimination, Nanosized hydroxyapatite, Oxalic acid, Solid phase extraction

INTRODUCTION

Organic acids are low molecular weight (LMW) compounds containing one or more carboxyl groups, which are common and natural constituents in many plants. Analysis of these organic acids has become increasingly important due to their role in the physiological activity of plants.[1]

Correspondence: Prof. Zhenggui Wei, College of Resources and Environmental Sciences, Nanjing Agricultural University, Nanjing 210095, P.R. China. E-mail: zgwei@njau.edu.cn

Some organic acids like citric, malic, succinic, and oxalic acids are parts of intermediates in the Krebs cycle, which is a central energy yielding cycle of the cell. Many of them are believed to play an important role in the cation transport (either nutrient or toxic) in xylem vessels.[2,3] In addition, low molecular weight organic acids like citric, oxalic, and malic acids are commonly released from plant roots that can form sufficiently strong complexes with Al^{3+} to resist its toxicity.[4–9] Moreover, as the simplest dicarboxylic acid in plants, oxalic acid in the xylem saps may have great importance during the long distance transportation and accumulation of heavy metals like cadmium[10–12] and uranium.[13] The success in clarification of these functions depend on the separation and identification of organic acids in different parts of plants.

Several methods have been reported for the separation and determination of oxalic acid in plant samples, including gas chromatography (GC), ion chromatography (IC), and reversed phase high performance liquid chromatography (RP-HPLC). As low molecular weight organic acids are generally non volatile, their determinations with GC require a derivatisation step, which is often quite tedious, time consuming, and retards the reproducibility of the analysis.[14] IC can be used to determine all the organic and inorganic anions. However, concentrations of inorganic anions (nitrate, sulfate, and phosphate) are often higher than those of organic anions (oxalate, malate, and citrate) in the xylem saps, high concentrations of sulfate ions have a severe interference on the determination of oxalic acid.[15] Recently, RP-HPLC is widely used for the determination of low molecular weight organic acids in plant parts and foods because of the simplicity, rapidity, and stability of the method.[16–19] Even though sulfate and phosphate ions have no ultraviolet absorbency, the existence of high concentrations of nitrate ions in the xylem saps have significant ultraviolet absorbency at 214 nm, which gives a large unretained peak, which can mask the first eluting oxalic acid,[20–22] despite the type of eluent, organic modifier, flow rate, column temperature, and ion pair (IP) reagent;[3] the results are still unsatisfactory. Therefore, in order to achieve accurate and reliable results, an efficient method to separate oxalic acid and eliminate the interference from nitrate ions is needed. Numerous substances have been proposed and used as sorbents in the separation and preconcentration of inorganic compounds, such as cation exchangeable resin,[23] active carbon,[24] modified silica,[25] alumina,[26] titanium dioxide,[27] but there are few reports on the separation of organic acids.

Nanosized materials are new solid materials made of nanoparticles that gained importance in recent years for their special properties. One of the unique properties of nanosized materials is that most of the atoms are on the surface; the surface atoms are unsaturated and can, therefore, bind with other atoms, and possess highly chemical activity.[28,29] Hydroxyapatite [HAP, $Ca_{10}(PO_4)_6(OH)_2$] is a major mineral component of

mammalian bones and teeth. It has been widely used, not only in biomedical applications, but also in separation and purification of proteins and other biomolecules.[30–32] Nanosized hydroxyapatite powders exhibit greater surface area and adsorption properties compared to bulk materials. However, there are few reports of the separation of low molecular weight organic acids and inorganic acid with nanosized hydroxyapatite.

In this work, we developed a new method using solid phase extraction with nanosized hydroxyapatite for solving interference from nitrate ion on oxalic acid in RP-HPLC. The optimum experimental conditions for the separation and determination of oxalic acid were studied in detail. The adsorption mechanism of oxalic on nanosized hydroxyapatite was elucidated by Fourier transform infrared (FT-IR) spectroscopy and X-ray diffraction (XRD) analyses. Finally, the proposed method was successfully employed for the determination of oxalic acid in the xylem saps of tomato plants.

EXPERIMENTAL

Reagents and Standard Solutions

All reagents used were of analytical-reagent grade. Oxalic, malic, and citric acids were obtained from Sinopharm Group Chemical Reagent Co., Ltd (Shanghai, China), and the other reagents were purchased from Nanjing Chemical reagent company (Nanjing, China). Deionized water from a Milli-Q water purification system was used for all solutions, dilution, and the mobile phase.

Stock standard solutions were prepared by dissolving organic acids in Milli-Q water, these solutions remained stable for several weeks if kept refrigerated at 4°C. The stock solution was diluted to obtain standard solutions in concentration ranges of 0.1–5.0 mmol/L for oxalic acid and 0.1–10.0 mmol/L for malic acid and 1.0–20 mmol/L for citric acid.

Plant Material and Collection of Plant Xylem Sap Samples

Tomato (*Lycopersicon esculentum*) seeds were germinated in the dark at 25°C in Petri dishes on wet filter paper for 3 days. The plants were cultivated in hydroculture in a green house with supplementary light to provide a 16 h photoperiod and with the temperature controlled at 25°C. The hydroculture solution contained 1.25 mmol/L KNO_3, 1.25 mmol/L $Ca(NO_3)_2$, 0.5 mmol/L $MgSO_4$, 0.25 mmol/L KH_2PO_4, 11.6 μmol/L H_3BO_3, 4.5 μmol/L $MnCl_2$, 10 μmol/L Fe-EDTA, 0.19 μmol/L $ZnSO_4$, 0.12 μmol/L Na_2MoO_4, 0.08 μmol/L $CuSO_4$, pH 5.5, adjusted with

H_2SO_4. The hydroculture solutions were aerated continuously and replaced every 3 days to prevent nutrient depletion and pH change. Xylem saps were collected from 6 to 8 week old plants, according to the method described by Wei et al.[15] The plants were cut with a sterilized razor blade just below the cotyledon internode, and then the decapitated stumps were fitted with a test tube (10 mL) maintaining negative pressure by means of a hand operated vacuum pump. During the suction procedure, the collected saps in the test tube were maintained at <4°C. The saps were collected for 2 h and filtered on a 0.45 μm Millipore filter before further use.

Apparatus and Chromatographic Conditions

The hydroxyapatite samples were analyzed by Fourier transform infrared (FT-IR) spectroscopy (Tensor 27, Bruker, Germany) as KBr pellets to confirm the phase formation. The crystallinity and purity of the mineral phases were determined by powder X-ray diffraction (XRD) on a Rigaku diffractometer (Rigaku D/max IIIB, Rigaku Co., Tokyo, Japan) with Cu Kα radiation (30 kV, 25 mA, $\lambda = 1.5405$ Å).

The HPLC analyses were carried out on a LC-20AT Shimadzu liquid chromatograph equipped with a SPD-20A Shimadzu UV-Vis detector (Shimadzu Co., Kyoto, Japan). Chromatographic conditions for reversed phase HPLC: a reversed phase C_{18} (Shim-pack VP-ODS 250 × 4.6 mm, 5 μm particle size) column connected with a C_{18} (Shim-pack GVP-ODS 210 × 4.6 mm, 5 μm particle size) guard column were used. The detector signal was recorded on a HW-2000 chromatographic workstation. The mobile phase was a buffer solution containing 5.0 g/L $(NH_4)_2HPO_4$ adjusted to pH 2.5 with H_3PO_4 and was filtered through a 0.45 μm membrane filter supplied by XinYa Corporation. (Shanghai, China). This mobile phase must be prepared fresh daily. The optimum wavelength for determination was 214 nm with a sensitivity of 0.1 absorbance unit, full scale. The flow rate was 1.0 mL/min. The injection volume was 20 μL and each sample was injected in triplicate. The determination of acids was done in peak area mode.

Analytical Procedures

The nanosized hydroxyapatite powders used to separate oxalic acid and nitrate ions were synthesized by a sol-gel method using $Ca(NO_3)_2 \cdot 4H_2O$ and $NH_4H_2PO_4$ as starting materials and ammonia solution as agents for pH adjustment, EDTA served as complex reagent.[33,34]

The adsorption behaviors of oxalic acid and nitric acid on the nanosized hydroxyapatite absorbent were studied in detail to get the optimum

separation conditions. Preliminary experiments showed that nitric acid could not be adsorbed by nanosized hydroxyapatite despite the pH, contact time, initial concentration, and the amount of nanosized hydroxyapatite was taken into consideration (data not shown). Oxalic acid can be adsorbed quantitatively after 60 minutes contact with nanosized hydroxyapatite at initial pH 2.5, and then oxalic acid was desorbed quantitatively from nanosized hydroxyapatite with 0.1 mol/L $(NH_4)_2HPO_4$, and it was determined by RP-HPLC at the optimum chromatographic conditions.

The adsorption capacity of oxalic acid on nanosized hydroxyapatite was determined by repeating the adsorption step recommended by M.S. Gasser.[35] Suspensions containing 0.1 g nanosized hydroxyapatite and 10 mL 5.0 mmol/L oxalic acid solution were placed in a horizontal shaker set at 200 rpm, and after a specified time, the suspensions were centrifuged at 3000 rpm for 10 min and filtered through a 0.45 μm Millipore filter, the two phases were separated, the filtrates were used for the RP-HPLC analysis, and the same adsorbent was used again with fresh oxalic acid solution. These procedures were repeated until no further uptake was observed. The solid residue with the maximum amount of oxalic acid adsorbed was analyzed by XRD and FT-IR in order to elucidate the adsorption mechanism of oxalic acid on nanosized hydroxyapatite.

The xylem sap samples were treated with the optimum separate conditions. First, the samples were diluted with deionized water in a ratio of 1:5, and adjusted to pH 2.5 with H_2SO_4, then 0.1 g nanosized hydroxyapatite was shaken with ten microliters of the diluted solution for 60 minutes at room temperature, after this, the nanosized hydroxyapatite loaded with oxalic acid was shaken with 0.1 mol/L $(NH_4)_2HPO_4$ for 120 minutes, to ensure the oxalic acid was desorbed completely, finally, the oxalic acid desorbed was determined by RP-HPLC at the optimum chromatographic conditions.

RESULTS AND DISCUSSION

Characteristics of Nanosized Hydroxyapatite

Previous reports clearly demonstrated that infrared spectroscopy was an indispensable tool in order to learn some special features of the synthetic hydroxyapatite.[36–39] Therefore, Fourier transform infrared characterization was carried out for both hydroxyapatite samples and the solid residue saturated with oxalic acid to study the spectral characteristics indicative of the chemical bonding.[40,41]

Figure 1 (A) shows the FT-IR spectrum of the synthetic hydroxyapatite samples. The IR bands at 3572 and 632 cm^{-1} belong to the vibration

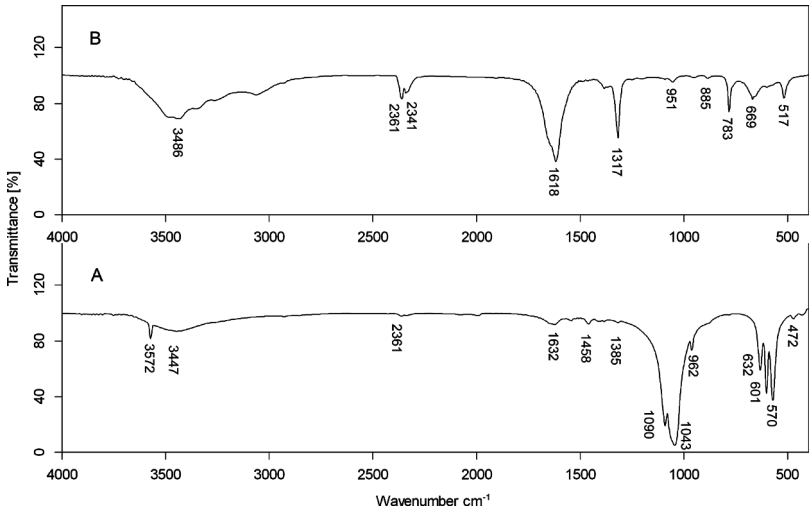

Figure 1. FT-IR spectrum of the synthetic hydroxyapatite before (A) and after (B) saturated with oxalic acid.

of hydroxyl, the bands at 1090, 1043, and 962 cm^{-1} are characteristic of the phosphate stretching vibration, and the bands observed at 601, 570, and 472 cm^{-1} are due to the phosphate bending vibration, the broad peaks at 1632 cm^{-1} and 3447 cm^{-1} are due to adsorbed water. Moreover, the trace carbonate ion peaks are very weak at 1385 and 1458 cm^{-1}. These indicate that the quality of our synthetic hydroxyapatite is excellent.

The FT-IR results obtained are completely consistent with the crystallization process observed by XRD measurements. The XRD pattern of synthetic hydroxyapatite is shown in Figure 2 (A), the prepared samples are in good agreement with the Powder Diffraction File ($Ca_{10}(PO_4)_6(OH)_2$, PDF Card No. 09–0432), and no characteristic peaks of impurities, such as calcium hydroxide and calcium phosphates, are observed, meaning that pure and well crystallized samples are obtained under the present experimental conditions. By applying the Scherrer formula to the full width at half maximum of the diffraction peaks,[42] we can calculate the average particle sizes of $Ca_{10}(PO_4)_6(OH)_2$ as 57.4 nm.

Optimization of Separation Conditions

Our particular interest focuses on the development of an effective method to eliminate the interference from nitrate ions to oxalic acid in RP-HPLC,

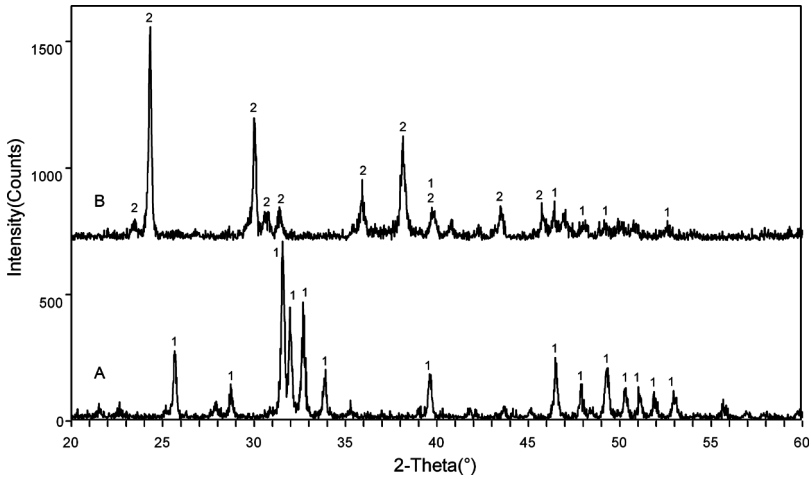

Figure 2. XRD patterns of the synthetic hydroxyapatite before (A) and after (B) saturated with oxalic acid. Peaks labeled "1" and "2" correspond to HAP (PDF Card No. 09-0432) and COM (PDF Card No. 20-0231), respectively.

it is, therefore, essential to investigate the adsorption and desorption behavior of oxalic acid on nanosized hydroxyapatite.

Adsorption Studies

As nitric acid cannot be adsorbed by nanosized hydroxyapatite, the influences of different parameters such as solution pH, equilibration time, initial oxalic acid concentration, and the amount of nanosized hydroxyapatite sorbents on the adsorption of oxalic acid are studied and discussed. As shown in Figures 3–6, the pH value plays an important role with respect to the adsorption of oxalic acid on the nanosized hydroxyapatite surface, it can be seen that the adsorption percent of oxalic acid decreases continuously with increasing pH, oxalic acid is adsorbed poorly at $pH > 8.0$. A quantitative adsorption (>95%) is found in the pH range of 2.0–4.0, after 60 minutes of contact time at the initial pH 2.0–3.0, oxalic acid in the solution can be adsorbed completely. The results can be explained as follows: the nanosized hydroxyapatite was partly dissolved at low pH, oxalic acid is adsorbed by hydroxyapatite through the coordination between calcium and oxalate, and this has been validated by the FT-IR and XRD analyses.

Figure 1 (B) shows the FT-IR spectrum of the solid residue with the maximum amount of oxalic acid adsorbed, compared to Figure 1 (A), the main peaks for PO_4^{3-} disappeared, and main antisymmetric carbonyl

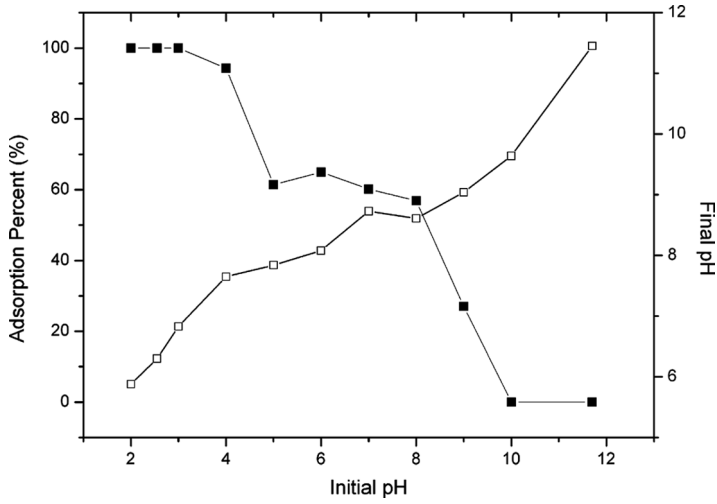

Figure 3. Effect of pH on the adsorption of oxalic acid onto nanosized hydroxyapatite.

stretching band at 1618 cm^{-1} and the metal-carboxylate stretch appears at 1317 cm^{-1}, are attributed to oxalate. The peak at 517 cm^{-1} arises due to O-C-O in-plane bending. The broad band around 3486 cm^{-1}

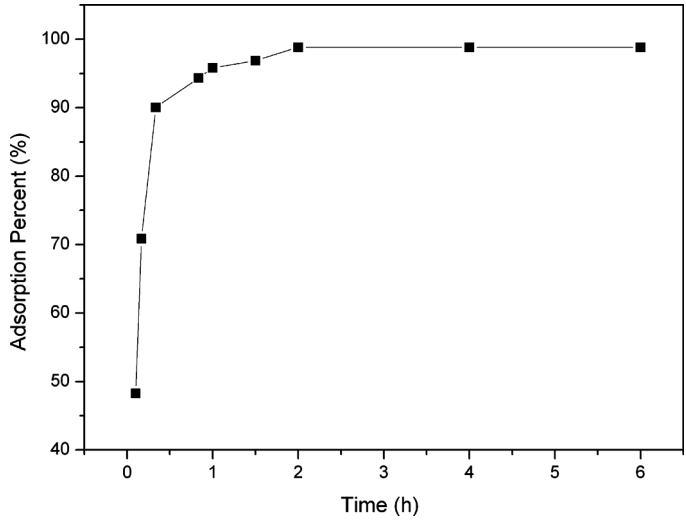

Figure 4. Effect of contact time on the adsorption of oxalic acid onto nanosized hydroxyapatite.

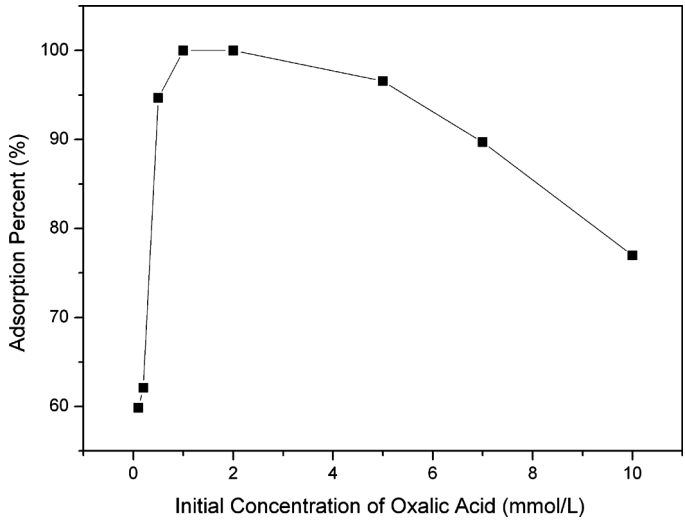

Figure 5. Effect of initial concentration on the adsorption of oxalic acid onto nanosized hydroxyapatite.

corresponds to the coordinated water molecules, while an out-of-plane bending band of water appears at 783 cm^{-1}. Moreover, the secondary absorption bands at 951 cm^{-1}, 885 cm^{-1}, and 669 cm^{-1} also due to the

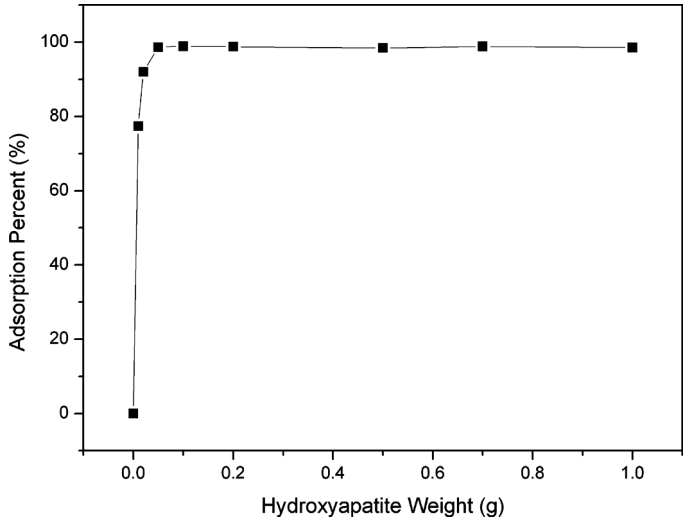

Figure 6. Effect of amount of nanosized hydroxyapatite on the adsorption of oxalic acid.

existence of calcium oxalate.[43] Thus, according to the stretching frequencies observed, the possible formation of crystalline calcium oxalate could be suggested.

The obtained FT-IR results are consistent with the XRD analyses. Figure 2 (B) shows the XRD pattern of the solid residue with the maximum amount of oxalic acid adsorbed, which matches exactly with the Powder Diffraction File (PDF Card No. 20–0231), and no other calcium phosphate phases can be detected. So we can further confirm that the new phase formed is Calcium oxalate monohydrate (COM).

Desorption Studies

The desorption of oxalic acid from nanosized hydroxyapatite are studied as shown in Figures 7–8. Preliminary experiments showed that 0.1 mol/L $(NH_4)_2HPO_4$ was suitable for desorption of oxalic acid. Thus, the nanosized hydroxyapatite loaded with oxalic acid is treated with the 10.0 mL of 0.1 mol/L $(NH_4)_2HPO_4$ solution on a horizontal shaker. The influences of contact time and solution pH are studied. It is clear that oxalic acid cannot be desorbed at $pH < 6.0$, the desorption percent increases sharply above pH 6.0, and has a complete desorption at pH 8.0. Therefore, a pH of 8.0 is selected as the compromise condition, and 2 h has proven to be enough for the desorption of oxalic acid.

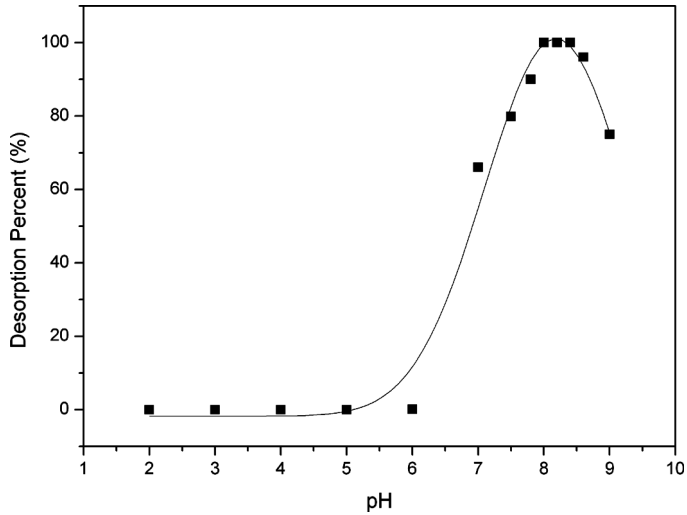

Figure 7. Effect of pH on the desorption of oxalic acid by 0.1 mol/L $(NH_4)_2HPO_4$.

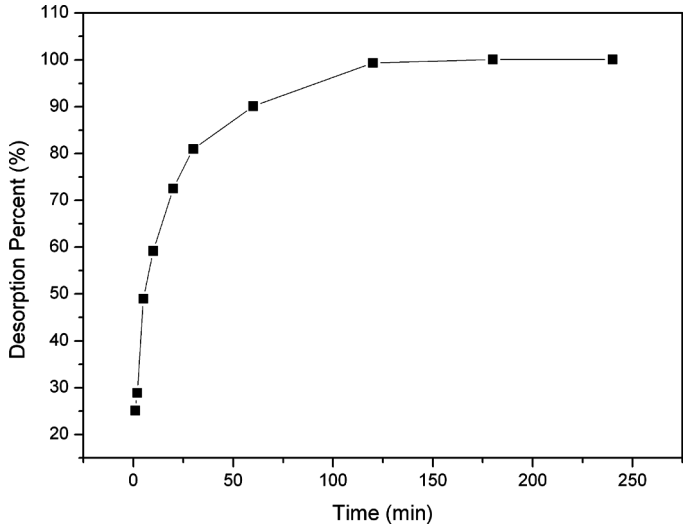

Figure 8. Effect of contact time on the desorption of oxalic acid by 0.1 mol/L $(NH_4)_2HPO_4$.

Optimization of Chromatographic Conditions

The oxalic acid was identified by comparison of the retention time with that of standard. An external calibration method with freshly prepared mixed standard solutions was used for quantitative determination of the acids. Figure 9 shows the chromatogram of a mixed standard solution with three organic acids (oxalic acid, malic acid, citric acid) being separated and identified by this method. The typical chromatogram of the xylem sap of tomato is shown in Figure 10. We can see the determination of oxalic is impossible, due to the presence of nitrate ions in high concentrations in the saps. Moreover, Tartár et al.[3] separated organic acids in xylem saps of tomato on a Nucleosil C18 column at a flow rate of 0.5 mL/min using tetrabutylammonium hydrogen sulfate ($TBAHSO_4$) dissolved in the mobile phase as ion-pairing (IP) regent; Senden et al.[21] separated organic acids in xylem saps of tomato by ion suppression RP-HPLC. But, the common defect is neither the separation of oxalic acid nor the identification in the samples, which could be carried out due to the presence of high concentrations of nitrate ions. Oxalic acid and nitrate ions are separated in this study. Figure 11 shows the chromatogram of oxalic acid in the xylem saps of tomato determined by RP-HPLC after the elimination of nitrate ions by the method presented in this paper.

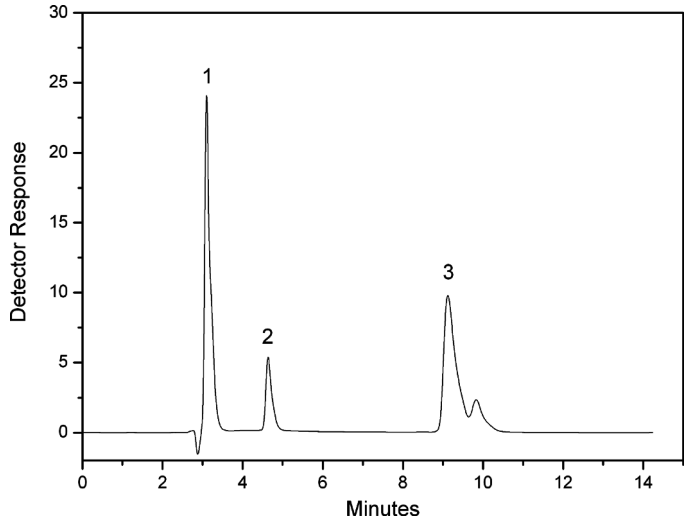

Figure 9. RP-HPLC chromatogram of a standard mixture of three organic acids. Peaks: 1 = oxalic acid, 2 = malic acid, 3 = citric acid.

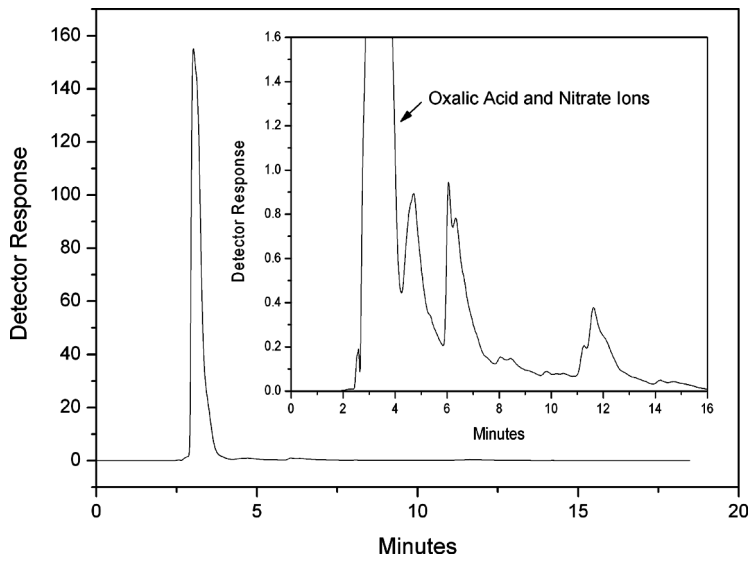

Figure 10. RP-HPLC chromatogram of organic acids in the xylem saps of tomato.

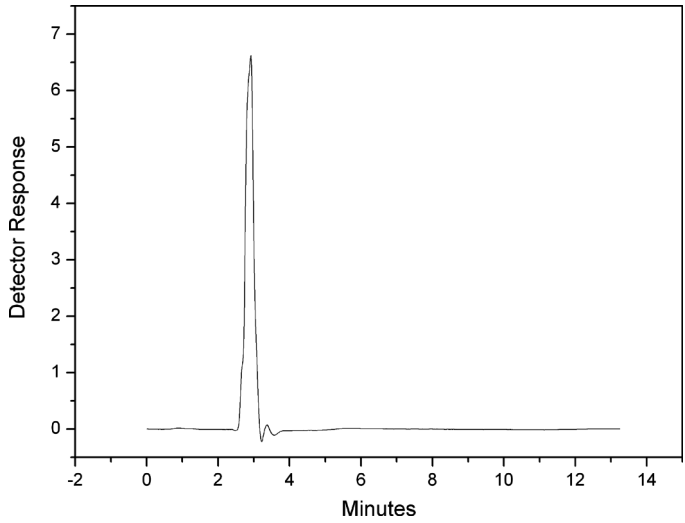

Figure 11. RP-HPLC chromatogram of oxalic acid in the xylem saps of tomato after the interference of nitrate ions is eliminated.

Influence of the Column Temperature

The column was controlled by a thermostat in several different temperatures and the best results were obtained at a temperature of 25°C.

Influence of Mobile Phase

The phosphate buffer solution was widely used as the mobile phase for the determination of organic acids.[3,20,28,29] Different concentrations of the phosphate buffer solution have a direct effect on the buffer capability. Furthermore, the concentrations can affect the forms of organic acids in the mobile phase and the ion intensity and, consequently, the separation effect of the chromatographic column. Several concentrations of $(NH_4)_2HPO_4$ were tested, and finally 5.0 g $(NH_4)_2HPO_4$ in the mobile phase was selected.

Influence of Mobile Phase pH and Flow Rate

Several mobile phase flow rates (0.5–1.5 mL/min) and pH values between 2.0 and 3.0 were tested, and finally, pH 2.5 and a flow rate of 1.0 mL/min were selected. Several wavelengths from 200 to 240 nm were tested, and finally, the optimum wavelength for determination was 214 nm.

Table 1. Detection and quantification limits of organic acids analyzed

Organic acid	Detection limit (mmoL/L)	Quantification limit (mmoL/L)
Oxalic	0.0004	0.0006
Malic	0.012	0.022
Citric	0.0069	0.013

Performance Characteristics of the Proposed Method

Optimized separation conditions and chromatographic conditions were set and the following analytical characteristics were evaluated: detection and quantification limits, calibration curves, precision and recovery, analysis of oxalic acid in the xylem saps of tomato.

Detection and Quantification Limits

The detection limit was calculated as $s_b + 3s$, where s_b was the average signal of 10 blank injections and s was the standard deviation. The quantification limit was calculated as $s_b + 10s$.[44] Table 1 shows the detection and quantification limits of organic acids analyzed by RP-HPLC. The detection limits ranged from 0.0004 mmol/L for oxalic acid to 0.0069 mmol/L for citric acid and the quantification limits ranged from 0.0006 mmol/L for oxalic acid to 0.022 mmol/L for malic acid.

Calibration Curves

Calibration curves were determined for six different concentrations of standard solutions for each organic acid analyzed. Each calibration sample was injected in triplicate. Calibration graphs for each compound were obtained by plotting concentration against peak area and applying the

Table 2. Parameters and correlation coefficients (r^2) of calibration plots for organic acids analyzed. Calibration plots are expressed as regression lines ($y = ax + b$), where y is the peak area and x is the amount of organic acids. The calibration test was repeated three times

Organic acid	a	b	r^2
Oxalic acid	0.9672	0.1402	0.9995
Malic	0.1850	0.0024	0.9999
Citric	0.3449	0.0065	0.9999

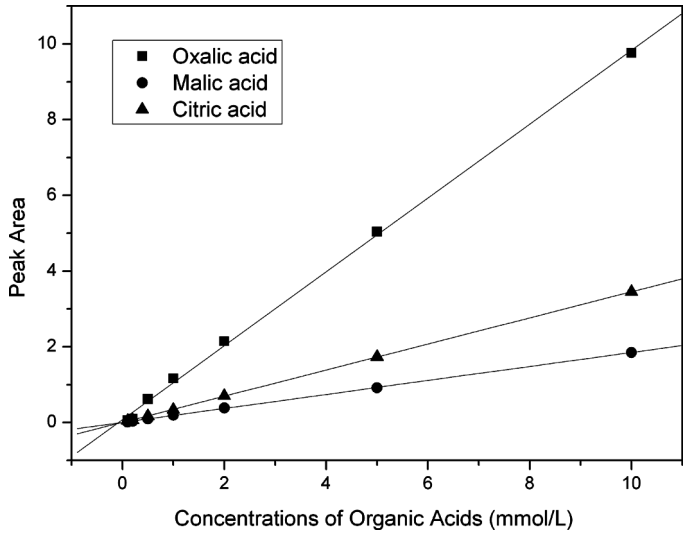

Figure 12. Calibration curves of organic acid standards.

least squares method. Table 2 shows the parameters and correlation coefficients of the calibration plots. Each plot was linear over a wide interval from the detection limit to at least 5.0 mmol/L for oxalic acid, 10.0 mmol/L for malic acid and citric acid. Calibration curves are shown in Figure 12.

Precision and Recovery

Under the optimum conditions, the reproducibility was established by injecting the xylem sap samples three times, and the relative standard deviations were less than 3.0%. The recoveries of the oxalic acid added to xylem sap samples were between 94.8% and 99.3%.

Table 3. Concentration of the oxalic acid in the xylem saps of tomato (Lycopersicon esculentum)

Organic acid	Original (mmoL/L)	Added (mmoL/L)	Found (mmoL/L)	Recovery (%)	RSD (%)
Oxalic acid	1.749	0.500	2.133	94.8	3.0
		1.00	2.708	98.5	2.8
		2.000	3.725	99.3	2.2

Analysis of Oxalic Acid in the Xylem Saps of Tomato

Oxalic acid in the xylem saps of tomato has been determined according to the steps described in the analytical procedures. The analytical results are shown in Table 3. As can be seen, this is a reliable method for the determination of oxalic acid in the xylem saps of tomato. It is the first time that the interference from high concentrations of nitrate ions on oxalic acid in RP-HPLC is eliminated by solid phase extraction with nanosized hydroxyapatite.

CONCLUSIONS

The interference from nitrate ions on oxalic acid in RP-HPLC is avoided by solid phase extraction with nanosized hydroxyapatite. High concentrations of nitrate ions are eliminated as they cannot be adsorbed by hydroxyapatite, by contrast, oxalic acid can be adsorbed completely within 60 minutes at initial pH 2.5, and then the oxalic acid retained is eluted from nanosized hydroxyapatite with 0.1 mol/L $(NH_4)_2HPO_4$. Recoveries for oxalic acid are from 94.8% to 99.3%. The near complete removal of nitrate ions from the samples by solid phase extraction with nanosized hydroxyapatite results in no interference of nitrate ions on oxalic acid in RP-HPLC. Meanwhile, the adsorption mechanism of oxalic acid on nanosized hydroxyapatite is proven to be the coordination between oxalate and calcium, by the results of FT-IR and XRD analyses. In conclusion, the proposed method is simple, effective, and reliable for the determination of oxalic acid in the xylem saps of tomato, and can be adapted to other plant samples.

ACKNOWLEDGMENT

This work is supported by National Programs for High Technology Research and Development of China (No. 2007AA10Z406), the Research Fund for the Dectoral Program of Higher Education (No. 20070307051), and the Foundation for Talent Recommendation Program of Nanjing Agricultural University (No. 030-804076).

REFERENCES

1. Rivasseau, C.; Boisson, A.M.; Mongélard, G.; Couram, G.; Bastien, O.; Bligny, R. Rapid analysis of organic acids in plant extracts by capillary electrophoresis with indirect UV detection Directed metabolic analyses during metal stress. J. Chromatogr. A **2006**, *1129* (6), 283–290.

2. Wang, M.; Qu, F.; Shan, X.Q.; Lin, J.M. Development and optimization of a method for the analysis of low-molecular-mass organic acids in plants by capillary electrophoresis with indirect UV detection. J. Chromatogr. A **2003**, *989* (2), 285–292.
3. Tatär, E.; Mihucz, V.G.; Kmethy, B.; Záray, G.; Fodord, F. Determination of organic acids and their role in nickel transport within cucumber plants. J. Microchem. **2000**, *67* (1–3), 73–81.
4. Ma, J.F.; Zheng, S.J.; Matsumoto, H.; Hiradate, S. Detoxifying aluminium with buckwheat. Nature **1997**, *390* (6660), 569–570.
5. Ma, J.F.; Ryan, P.R.; Delhaize, E. Aluminium tolerance in plants and the complexing role of organic acids. Trends Plant Sci. **2001**, *6* (6), 273–278.
6. Ma, Z.; Miyasaka, S.C. Oxalate Exudation by Taro in Response to Al. Plant Physiol. **1998**, *118* (3), 861–865.
7. Ma, J.F.; Hiradate, S.; Matsumoto, H. High aluminum resistance in buckwheat: II. Oxalic acid detoxifies aluminum internally. Plant Physiol. **1998**, *117* (3), 753–759.
8. Delhaize, E.; Ryan, P.R. Aluminum toxicity and tolerance in plants. Plant Physiol. **1995**, *107* (2), 315–321.
9. Li, X.F.; Ma, J.F.; Matsumoto, H. Pattern of aluminum-induced secretion of organic acids differs between rye and wheat. Plant Physiol. **2000**, *123* (4), 1537–1543.
10. Krishnamurti, G.S.R.; Cieslinski, G.; Huang, P.M.; Van Rees, K.C.J. Kinetics of cadmium release from soils as influenced by organic acids: implication in cadmium availability. J. Environ. Qual. **1997**, *26* (1), 271–277.
11. Ciesliński, G.; Van Rees, K.C.J.; Szmigielska, A.M.; Krishnamurti, G.S.R.; Krishnamurti, G.S.R.; Huang, P.M. Low-molecular-weight organic acids in rhizosphere soils of durum wheat and their effect on cadmium bioaccumulation. Plant and Soil. **1998**, *203* (1), 109–117.
12. Senden, M.H.M.N.; van der Meer, A.J.G.M.; Verburg, T.G.; Wolterbeek, H.Th. Citric acid in tomato plant roots and its effect on cadmium uptake and distribution. Plant and Soil. **1995**, *171* (2), 333–339.
13. Huang, J.W.; Michael, J.; Blaylock; Kapunik, Y.; Ensley, B. Phytoremediation of uranium-contaminated soils: role of organic acids in triggering uranium hyperaccumulation in plants. Environ. Sci. Technol. **1998**, *32* (13), 2004–2008.
14. Morvai, M.; Molnár-Perl, I.; Knausz, D. Simultaneous gas liquid chromatographic determination of sugars and organic acids as trimethylsilyl derivatives in vegetables and strawberries. J. Chromatogr. A. **1991**, *552* (9), 337–344.
15. Wei, Z.G.; Wong, J.W.; Hong, F.S.; Zhao, H.Y.; Li, H.X.; Hu, F. Determination of inorganic and organic anions in xylem saps of two contrasting oilseed rape (Brassica juncea L.) varieties: roles of anions in long-distance transport of cadmium. J. Microchem. **2007**, *86* (1), 53–59.
16. Lian, H.Z.; Mao, L.; Ye, X.L.; Miao, J. Simultaneous determination of oxalic, fumaric, maleic and succinic acids in tartaric and malic acids for pharmaceutical use by ion-suppression reversed-phase high performance liquid chromatography. J. Pharm. Biomed. Anal. **1999**, *19* (3–4), 621–625.

17. Rodrigues, C.I.; Martaa, L.; Maiaa, R.; Mirandab, M.; Ribeirinhob, M.; Máguas, C. Application of solid-phase extraction to brewed coffee caffeine and organic acid determination by UV/HPLC. J. Food Compos. Anal. **2007**, *20* (5), 440–448.
18. Ding, J.H.; Wang, X.X.; Zhang, T.L.; Li, Q.M.; Luo, M.B. Optimization of RP–HPLC Analysis of Low Molecular Weight Organic Acids in Soil. J. Liq. Chromatogr. & Rel. Technol. **2006**, *29* (1), 99–112.
19. Cunha, S.C.; Fernandes, J.O.; Isabel, M.P.L.V.O. Ferreira. HPLC/UV determination of organic acids in fruit juices and nectars. Eur. Food Res. Technol. **2002**, *214* (1), 67–71.
20. Tatär, E.; Mihucz, V.G.; Kmethy, B.; Záray, G.; Fodord, F. Determination of Organic Acids in Xylem Sap of Cucumber: effect of lead contamination. J. Microchem. **1998**, *58* (3), 306–314.
21. Senden, M.H.M.N.; Vander Meer, A.J.G.M.; Limborgh, J.; Wolterbeek, H.Th. Analysis of major tomato xylem organic acids and PITC-derivatives of amino acids by RP-HPLC and UV detection. Plant and Soil. **1992**, *142* (1), 81–89.
22. Touraine, B.; Astruc, S. Purification and dual-column HPLC determination of carboxylic acids in tissues, phloem and xylem saps of soybean plants. Chromatographia. **1990**, *30* (7–8), 388–392.
23. Cao, X.; Yin, M.; Wang, X. Elimination of the spectral interference from polyatomic ions with rare earth elements in inductively coupled plasma mass spectrometry by combining algebraic correction with chromatographic separation. Spectrochim. Acta, Part B. **2001**, *56* (4), 431–441.
24. Narina, I.; Soylak, M.; Elcib, L.; Doganc, M. Determination of trace metal ions by AAS in natural water samples after preconcentration of pyrocatechol violet complexes on an activated carbon column. Talanta. **2000**, *52* (6), 1041–1046.
25. Matoso, E.; Kubota, L.T.; Cadore, S. Use of silica gel chemically modified with zirconium phosphate for preconcentration and determination of lead and copper by flame atomic absorption spectrometry. Talanta. **2003**, *60* (6), 1105–1111.
26. Hiraide, M.; Iwasawa, J.; Kawaguchi, H. Collection of trace heavy metals complexed with ammonium pyrrolidinedithiocarbamate on surfactant-coated alumina sorbents. Talanta. **1997**, *44* (2), 231–237.
27. Vassileva, E.; Proinova, I.; Hadjiivanov, K. Solid-phase extraction of heavy metal ions on a high surface area titanium dioxide (anatase). Analyst. **1996**, *121*, 607–612.
28. Liang, P.; Hu, B.; Jiang, Z.C.; Qin, Y.C.; Peng, T.Y. Nanometer-sized titanium dioxide micro-column on-line preconcentration of La, Y, Yb, Eu, Dy and their determination by inductively coupled plasma atomic emission spectrometry. J. Anal. At. Spectrom. **2001**, *16*, 863–866.
29. Pu, X.L.; Jiang, Z.C.; Hu, B.; Wang, H.B. γ-MPTMS modified nanometer-sized alumina micro-column separation and preconcentration of trace amounts of Hg, Cu, Au and Pd in biological, environmental and geological samples and their determination by inductively coupled plasma mass spectrometry. J. Anal. At. Spectrom. **2004**, *19*, 984–989.

30. Vallet-Regí, M.; González-Calbet, J.M. Calcium phosphates as substitution of bone tissues. Prog. Solid State Chem. **2004**, *32* (1–2), 1–31.
31. Tiselius, A.; Hjertén, S.; Levin, Ö. Protein chromatography on calcium phosphate columns. Arch. Biochem. Biophys. **1956**, *65* (1), 132–155.
32. Schröder, E.; Jönsson, T.; Poole, L. Hydroxyapatite chromatography: Altering the phosphate-dependent elution profile of protein as a function of pH. Anal. Biochem. **2003**, *313* (1), 176–178.
33. Long, M.; Hong, F.S.; Li, W.; Li, F.C.; Zhao, H.Y.; Lv, Y.Q.; Li, H.X.; Hu, F.; Sun, L.D.; Yan, C.H.; Wei, Z.G. Size-dependent microstructure and europium site preference influence fluorescent properties of Eu^{3+}-doped $Ca_{10}(PO_4)_6(OH)_2$ nanocrystal. J. Lumin. **2008**, *128* (3), 428–436.
34. Liu, J.B.; Li, K.W.; Wang, H.; Zhu, M.K.; Yan, H. Rapid formation of hydroxyapatite nanostructures by microwave irradiation. Chem. Phys. Letts. **2004**, *396* (4–6), 429–432.
35. Gasser, M.S. Adsorption and pre-concentration of Gd(III) and U(VI) from aqueous solution using artificial adsorbents. Sep. Purif. Technol. **2007**, *53* (1), 81–88.
36. Han, J.K.; Song, H.Y.; Saito, F.; Lee, B.T. Synthesis of high purity nano-sized hydroxyapatite powder by microwave-hydrothermal method. Mater. Chem. Phys. **2006**, *99* (2–3), 235–239.
37. Wang, A.L.; Yin, H.B.; Liu, D.; Wu, H.X.; Ren, M.; Jiang, T.S.; Cheng, X.N.; Xu, Y.Q. Size-controlled synthesis of hydroxyapatite nanorods in the presence of organic modifiers. Mater. Letts. **2007**, *61* (10), 2084–2088.
38. Sonoda, K.; Furuzono, T.; Walsh, D.; Sato, K.; Tanaka. Influence of emulsion on crystal growth of hydroxyapatite. Solid. State Ionics. **2002**, *151* (1–4), 321–327.
39. Wang, Y.J.; Chen, K.W.; Zhang, S.H.; Wang, X.D. Surfactant-assisted synthesis of hydroxyapatite particles. Mater. Letts. **2006**, *60* (27), 3227–3231.
40. Bogdanoviciene, I.; Beganskiene, A.; Tõnsuaadu, K.; Glaser, J.; Jürgen Meyer, H.; Kareiva, A. Calcium hydroxyapatite, $Ca_{10}(PO_4)_6(OH)_2$ ceramics prepared by aqueous sol-gel processing. Mater. Res. Bull. **2006**, *41* (9), 1754–1762.
41. Smiciklas, I.; Onjia, A.; Raicevic, S. Experimental design approach in the synthesis of hydroxyapatite by neutralization method. Sep. Purif. Technol. **2005**, *44* (2), 97–102.
42. Zakeri, M.; Yazdani-Rad, R.; Enayati, M.H.; Rahimipour, M.R. Synthesis of nanocrystalline $MoSi_2$ by mechanical alloying. J. Alloys Comp. **2005**, *403* (1–2), 258–291.
43. Maurice-Estepa, L.; Levillain, P.; Lacour, B.; Daudon, M. Advantage of zero-crossing-point first-derivative spectrophotometry for the quantification of calcium oxalate crystalline phases by infrared spectrophotometry. Clin. Chim. Acta. **2000**, *298* (1–2), 1–11.
44. Suárez-Luque, S.; Matoa, I.; Huidobro, J.F.; Simal-Lozano, J.; Sancho, T. Rapid determination of minority organic acids in honey by high-performance liquid chromatography. J. Chromatogr. A. **2002**, *955* (2), 207–214.

Received May 23, 2008
Accepted June 23, 2008
Manuscript 6356